**Noname manuscript No.**
(will be inserted by the editor)

# A note on estimating $T_e$ from Bouguer coherence

**Dan** M$^{c}$Kenzie

Received:???

**Abstract** The coherence between Bouguer gravity anomalies and topography is widely used to estimate the value of $T_e$, the effective elastic thickness of the lithosphere. In areas where there is little topography but substantial free air gravity anomalies there is often little coherence between the free air anomalies and topography. In such regions the Bouguer coherence method generally gives estimates of $T_e$ of 90 km or more. A detailed analysis shows that, under these conditions, the value of the Bouguer coherence $\gamma_b^2$ is entirely controlled by the ratio of the power spectra of the free air gravity anomalies and the uncompensated topography, and contains no information about the value of $T_e$. What is worse, under these circumstances the variation of $\gamma_b^2$ with wavelength closely resembles that expected for large values of $T_e$. These results show that neither the Bouguer coherence method nor the admittance method can produce meaningful estimates of $T_e$ when the free air gravity anomalies are incoherent with the topography.

**Keywords** Bouguer coherence; Effective elastic thickness.

## 1 Introduction

An important constraint on lithospheric rheology is the value of $T_e$, its effective elastic thickness. In oceanic regions $T_e$ is usually estimated in the spectral domain, using the transfer function, often called the admittance, between the bathymetry taken as input and the free air gravity anomaly as output. Watts [13] reviews a number of such studies, which show that the value of $T_e$ increases from $\sim$ 3 km on slowly spreading ridges to more than 20 km beneath old cold lithosphere. In contrast, estimates of $T_e$ for continental regions are the subject of an ongoing controversy, which has recently been reviewed by Kirby [5]. Several approaches have been used to make estimates of $T_e$. Banks et al. [1] and McNutt and Parker [8] used the transfer function between Bouguer gravity anomalies and topography for the U.S. and Australia. They estimated the value of $T_e$ to be 6 and 1 km respectively. Forsyth [3] introduced a new method of estimating $T_e$ that used the coherence between Bouguer gravity anomalies and topography. Application of Forsyth's method

Department of Earth Sciences, Bullard Labs
Madingley Road, Cambridge CB3 0EZ, U.K.
Tel. +44 1223 337191
Fax +44 1223 360779
E-mail: mckenzie@madingley.org

to the shields of the U.S. (Bechtel et al. [2]) and Australia (Zuber et al. [14]) gave values of $T_e$ of 90 km or more for the parts of both regions that consist of shields. Such large values of $T_e$ are only possible if elastic stresses can be maintained for periods of 10–1000 Ma in mantle material whose temperature is $\sim 1000°$C. In contrast, in oceanic regions the base of the elastic layer is at a temperature of $\sim 450°$C (Watts [13]). Another constraint on lithospheric rheology is the thickness of the seismogenic layer, $T_s$, which is no more than $\sim 50$ km beneath both oceans and continents, and has a temperature of less than 600°C (Jackson et al. [4]). The seismogenic layer need only store elastic stresses for $\sim 1$ ka, and therefore its thickness is expected to be greater than $T_e$. This expectation is borne out in oceanic regions, but not in continental regions if $T_e$ is 90 km or more.

These problems caused McKenzie and Fairhead [7] and McKenzie [6] to examine in some detail the assumptions underlying Forsyth's approach. Forsyth assumed that the elastic layer was loaded in two ways, from the top and from the bottom. If the top load is incoherent with the bottom load, both loads must generate topography. However, in areas where there is little topography, the observed value of the coherence between the free air gravity and topography is often close to zero at all wavelengths. This lack of coherence must be taken into account, and provides the key to understanding why Forsyth's method generates such large estimates of $T_e$.

The standard admittance approach assumes that the Fourier transform of the observed free air gravity anomaly $\overline{g}^o_f$ is related to that of the topography $\overline{t}$ by

$$\overline{g}^o_f = Z^o(k)\overline{t} + \overline{n} \tag{1}$$

where $k = (k_x^2 + k_y^2)^{1/2}$ is the wavenumber, $Z^o$ is the transfer function, which is often called the admittance, and $\overline{n}$ is that part of $\overline{g}^o_f$ which is incoherent with the topography. $Z$ can then be obtained from

$$Z^o(k) = \frac{< \overline{g}^{o\star}_f \overline{t} >}{< \overline{t}^\star \overline{t} >} \tag{2}$$

where $^\star$ denotes complex conjugation, and the angle brackets averages over the semicircular annulus $k + \Delta k, k - \Delta k$ in the 2D spectral domain. The coherence $\gamma^2_f$ between the between the 2D Fourier transforms of the free air gravity and topography in the spectral domain is

$$\gamma^2_f(k) = \frac{< \overline{g}^{o\star}_f \overline{t} >^2}{< \overline{g}^{o\star}_f \overline{g}_f >< \overline{t}^\star \overline{t} >} \tag{3}$$

The misfit $H$ between the observed values of admittance $Z^o_i$ and those calculated from the flexural model $Z^c_i$ is given by

$$H(T_e) = \left[ \frac{1}{N} \sum_{i=1}^{N} \left( \frac{Z^o_i - Z^c_i(T_e)}{\sigma_i} \right)^2 \right]^{1/2} \tag{4}$$

where $\sigma_i$ is the standard deviation of $Z^o_i$, which depends on $\gamma^2_f$ (Munk and Cartwright [9]), and $Z^c_i$ is calculated from equation (11) with $F = 1$. The value of $T_e$ is also estimated from the Bouguer coherence, $\gamma^2_b$, calculated from equation (3) using $\overline{g}^o_b$ instead of $\overline{g}^o_f$ and Forsyth's approach.

Forsyth [3] considered two types of load, imposed at the surface or internally at the Moho. McKenzie [6] argued that internal loads should be separated into two types, depending on whether or not they were coherent with the surface topography. Loads with no surface expression must actually consist of both an internal and a surface load (see below). They result from erosion, which acts to remove surface topography and finally leaves a flat plain at sea level. However, erosion does not remove the subsurface density contrasts, which will still produce free air gravity anomalies when the surface is flat. If gravity could be switched off, removing all gravitational stresses, loads that now have no surface expression would then become associated with topography.

## 2 An Example

The gravity and topography of central and Western Australia provide an good illustration of the difficulties discussed above. Figs. 1a and 1b show the free air gravity anomalies and topography for Australia, and the box used to calculate the quantities in Fig. 2. As is commonly the case for regions underlain by old rocks and shields, there is little topography in central and Western Australia, though Fig. 1a shows that there are large gravity anomalies in this region.

Fig. 2 illustrates the results of applying the standard admittance approach described above to the data set from Australia shown in Fig. 1b. Because the free air coherence is so small, the values of $Z^o(k)$ are poorly determined. Fig. 2d shows that $H(T_e)$ has a shallow minimum at $T_e = 31.5$ km. However, the fit to the observations in Fig. 2a is unconvincing. Fig. 2c shows that the free air gravity anomalies are not, in general, coherent with the topography. As Zuber et al. [14] found, there is weak coherence between wavelengths of 200 and 300 km, and Fig. 2b shows that the phase of the admittance in this wavelength band is 180°. Therefore the free air gravity field is dominated by loads with no surface expression. This behaviour is commonly the case for shields. As Figs. 2a and 2d clearly show, it is not possible to obtain a useful estimate of $T_e$ using the admittance, because of the absence of coherence between the topography and the free air gravity. In contrast, Fig. 2e shows that the observed variations in Bouguer coherence give an estimate of $T_e \simeq 90$ km, in agreement with Zuber et al. [14].

The first issue is to examine the consequences of the lack of coherence between the free air gravity and the topography. Equation (3) shows that $\gamma_f^2 = 0$ requires

$$< \overline{g}_f^{o\star} \overline{t} >= 0 \tag{5}$$

The Bouguer gravity field $g_b^o$ can be constructed from $g_f^o$ and $t$

$$g_b^o = g_f^o - At \tag{6}$$

where $A$ is a constant. If gravity is measured in mGals, the topography in metres and its density is taken to be 2670 kg m$^{-3}$, then $A = 0.11194$. If there is no coherence between the free air gravity and topography, then equations (3), (5) and (6) require

$$\gamma_b^2(k) = \frac{A^2 < \overline{t}^\star \overline{t} >}{< \overline{g}_f^{o\star} \overline{g_f^o} > + A^2 < \overline{t}^\star \overline{t} >} = \frac{1}{1 + R(k)} \tag{7}$$

where

$$R(k) = \frac{< \overline{g}_f^{o\star} \overline{g_f^o} >}{< A\overline{t}^\star A\overline{t} >} \tag{8}$$

is the ratio of the power in the observed free air gravity field, $g_f^o$, to that of the gravity field from the surface topography, $At$, in the relevant wavenumber band. The Fourier transform of the free air gravity anomaly $\overline{g_f^o}$ would be given by $A\overline{t}$ if the surface topography was the only load and there was no compensation. Fig. 3a shows the Bouguer coherence $\gamma_b^2$ calculated from $R(k)$ using equations (7) and (8). As expected, the behaviour of $\gamma_b^2$ in Fig. 3a is similar to that in Fig. 2e, and yields a similar estimate of $T_e$. Fig. 3c shows the individual power spectra $< \overline{g}_f^{o\star} \overline{g}_f^o >$ and $< A\overline{t}^\star A\overline{t} >$. At wavelengths less than about 400 km the power of the gravity field calculated from the uncompensated topography is an order of magnitude less than that of the free air gravity. Therefore in this range of wavelengths the free air gravity must be dominated by internal loads and it is then not surprising that $\gamma_f^2$ is not significantly different from 0. At wavelengths greater than about 600 km $R < 1$ and equation (7) then shows that $\gamma_b^2 > 0.5$, even though $\gamma_f^2$ remains insignificant. This behaviour must result from isostatic compensation of the topography, since

otherwise the correlation between the topography and the free air gravity would be expected to be substantial.

This discussion shows that there is a serious problem with using the Bouguer coherence to estimate $T_e$ when $\gamma_f^2 \simeq 0$. If the topography in Fig. 1b is further reduced by erosion, the free air gravity field will scarcely change, because it is dominated by internal loads and its coherence with the topography is anyway insignificant. So erosion will reduce $< A\bar{t}^{\star} A\bar{t} >$ but leave $< \overline{g}_f^{o\star} \overline{g_f^o} >$ almost unaffected. The consequence of this behaviour is illustrated in Fig. 3b and 3c, where the topography in Fig. 1b has been reduced by a factor of 2. As expected from equation (7), this change increases the value of $R$ and hence the estimated value of $T_e$. Therefore the value of $T_e$ estimated from the Bouguer coherence is controlled by the power in the uncompensated topography, and will become arbitrarily large as the topography is removed by erosion. It is therefore meaningless.

Though this argument is formally correct it contains no physics, and in particular does not account for the incoherence between the free air gravity and the topography. A simple model that can do so was proposed by Forsyth [3], and consists of a crustal layer of constant thickness $d$ and density $\rho_c$, overlying a mantle with density $\rho_m$, the whole having an elastic thickness $T_e$. The plate is loaded by applying a layer of thickness $s_1$ and density $\rho_c$ to its surface, and another of thickness $s_2$ and density $\rho_m$ to the Moho. When $s_1$ and $s_2$ are uncorrelated Kirby [5] gives an expression for $\gamma_f^2$ which has been used to calculate the curves in Fig. 4 for various values of $f$, the ratio of the Moho load to the surface load, where

$$f = \frac{(\rho_m - \rho_c) s_2}{\rho_c s_1} \tag{9}$$

This plot shows that no choice of $f$ can generate $\gamma_f^2 \simeq 0$ at all wavelengths.

Since the topography is never completely flat, the observed lack of coherence at all wavelengths cannot be modelled if the surface and internal loads are incoherent with each other. It requires loads that are perfectly coherent with each other, and their ratio to be chosen so that there is no topography (McKenzie [6], Simons and Ohlede [12]). This is the essential difference between the model used below and that discussed by Forsyth [3] and Kirby [5]. Furthermore, if $\gamma_f^2 \simeq 0$, the gravity field from loads with no topographic expression must dominate that from the surface topography. If the coherence between $\overline{s}_1$ and $\overline{s}_2$ is 1, the resulting expression for the admittance $Z$ between the free air gravity and the topography is

$$\overline{g}_f^t = Z^c(k) \bar{t} \tag{10}$$

where

$$Z^c(k) = AG(k) \tag{11}$$

$$G(k) = \left[ 1 + \left( \frac{(1-F)(\psi+1) - rF}{rF(\zeta+1) - (1-F)} \right) \exp(-kd) \right] \tag{12}$$

and the crust is assumed to have the standard Bouguer density. $F$ is the fraction of the total load applied to the surface

$$F(k) = \frac{\rho_c \overline{s}_1}{\rho_c \overline{s}_1 + (\rho_m - \rho_c)\overline{s}_2} = \frac{1}{1+f} \tag{13}$$

and

$$\psi = \frac{Dk^4}{g\rho_c}, \qquad \zeta = \frac{Dk^4}{g(\rho_m - \rho_c)}, \qquad r = \frac{\rho_m}{\rho_c} - 1 \tag{14}$$

$g$ is the acceleration due to gravity, $d$ (= 35 km) the crustal thickness, $\rho_m$ (= 3300 kg m$^{-3}$) the mantle, and $\rho_c$ (= 2670 kg m$^{-3}$) the crustal, density. $D$ is the flexural parameter

$$D = \frac{ET_e^3}{12(1-\sigma^2)} \tag{15}$$

where $E(= 9.5 \times 10^{10}$ Pa) is Young's modulus and $\sigma(= 0.295)$ Poisson's ratio. The surface topography must always generate a free air gravity anomaly $g_f^t$. $1 > G(k) > 0$ is the factor by which the gravity field from the uncompensated topography is reduced by the effect of the compensation. At long wavelengths these expressions show that, as $k \to 0$, $\psi \to 0$, $\zeta \to 0$ and therefore $G \to 0$, irrespective of the value of $F$ and $D$. Therefore $R \to 0$ and $\gamma_b^2 \to 1$ as $k \to 0$, also irrespective of the values of $T_e$ and $D$. The effect of the finite value of $T_e$ is to reduce the power of the free air gravity anomaly expected from the topography. Fig. 5 shows three examples, all calculated with $F = 1$. The curve in Fig. 5a for $T_e = 90$ km gives gravity signal from the topography which has a similar magnitude to that observed between wavelengths of 600 and 1000 km. Therefore the gravity signal from the topography should make an important contribution to the free air gravity, even if there is also a contribution from subsurface density contrasts. It is then difficult to understand how $\gamma_f^2 \simeq 0$ in this wavelength range if $T_e$ is as large as 90 km. Values of $T_e$ of 30 and 10 km in Fig. 5b generate free air anomalies that have about an order of magnitude less power in this wavelength range than that observed, so it is less surprising that $\gamma_f^2 \simeq 0$. This behaviour therefore provides an upper bound on the value of $T_e$ of $\sim 30$ km.

Another issue is whether the free air gravity field can be used to estimate $T_e$ when it is dominated by loads with no surface expression. Such loads result from erosion, and are the dominant contributors to the free air gravity anomalies over most shields. This question can be addressed using the same simple flexural model. The value of $F(k)$ that generates a completely flat upper surface when $\overline{s}_1, \overline{s}_2 \neq 0$ is

$$F(k) = \frac{1}{r(\zeta + 1) + 1} \tag{16}$$

Fig. 6 shows curves for three values of $T_e$. These show that, by itself, the observation that $\gamma_f^2 \simeq 0$ does not provide a constraint on the likely value of $T_e$: It only does so when the power spectra of the free air gravity and topography are also known.

## 3 Other regions

The relationship between topography and gravity illustrated in Figs. 1 and 2 is common in old shield regions of the continents. Fig. 7 shows three other such regions where there is little coherence between topography and free air gravity anomalies. In all three regions Forsyth's method has been used to estimate $T_e$. In S. America Pérez-Gussinyé et al. [11] obtained values of $T_e$ of more than 70 km. In central N. America Bechtel et al. [2] estimated a value of $T_e$ of 82 km, and in central and eastern Europe Pérez-Gussinyé and Watts [10] obtained values of more than 70 km. These values agree well with those in Fig. 8 obtained from the regions shown in Fig. 7a. Because the coherence between the free air gravity and topography is close to zero in all three regions, the value of $\gamma_b^2$ is controlled by the ratio of the power spectra of the free air gravity to that of the uncompensated topography.

Unlike the Bouguer coherence method of estimating $T_e$, the admittance method does not suffer from the same confusion when there is no significant coherence between the free air gravity and the topography. Fig. 7b-d show that it cannot be used to estimate $T_e$ in any of these regions, because the coherence between the topography and the free air gravity anomalies is close to zero. In all cases $H(T_e)$ (not shown) is almost flat, as it is in Fig. 2d. However, Fig. 9 shows that in two cases, C. North America and NE Brazil, there is sufficient power in the topography to impose an upper bound on $T_e$ of $\sim 30$ km if the gravity signal from the surface topography is to be incoherent with the free air gravity. In contrast, the topography in E. Europe is too flat to provide any such bound.

## 4 Discussion

One reason for the popularity of the Bouguer coherence method of estimating $T_e$ is that it generates estimates where the admittance method fails. However, as discussion above shows, this apparent advantage is completely misleading when the topography has been strongly reduced by erosion. The only obvious indication that the Bouguer coherence method has failed is that the coherence between the free air gravity and topography is close to zero. When this happens neither method can produce reliable estimates. It is particularly unfortunate and misleading that the behaviour of $\gamma_b^2(k)$ can be fitted by selecting a value of $T_e$, even when the relationship between gravity and topography may in fact contain little or no information about its value.

When there is no significant coherence between the free air gravity and topography, estimates of $T_e$ can still be obtained by fitting profiles of free air gravity anomalies in the space domain. Estimates obtained in this way are considerably less accurate that those obtained in the spectral domain, and in particular the upper limits of $T_e$ are generally poorly constrained. Values obtained by this method are about 10 and 16 km for individual profiles from central Australia and the US respectively (McKenzie and Fairhead [7]), and 7 and 15 km for stacked profiles. These estimates are in general agreement with those of 10–33 km from similar cratonic regions that have rough topography, where the spectral approach can be used (McKenzie unpublished). Furthermore they are consistent with the upper bounds on $T_e$ obtained above, using the condition that the ratio of the power in the observed free air gravity to that from the surface topography should be large if $\gamma_f^2$ is to be small. As expected from the difference in the time scales, they are also less than the values of $T_s$.

What remains unclear is whether values of $T_e$ obtained from Bouguer coherence when $\gamma_f^2$ is substantial are estimates or simply upper bounds. In such regions the value of $T_e$ from Bouguer coherence is usually about a factor of two greater than that obtained from the admittance, and is also usually greater than $T_s$. Both observations suggest that it provides an upper bound rather than an estimate.

Simons and Olhede [12] have recently cast the problem of estimating $T_e$ into a modern statistical framework. Their approach uses Bouguer, rather than free air, anomalies, and hence requires the density of the topography to be known. They also assume that the ratio of the surface to the subsurface load is constant and independent of wavelength. However, this condition is not satisfied by loads with no surface expression (McKenzie [6], Simons and Olhede [12], equation 70). Such loads must be responsible for the behaviour of the coherence in Figs. 2c and 7b-d. Simons and Olhede show that their method works excellently on synthetic data, and it will be of great interest to discover whether a similar approach is equally successful on real data.

## 5 Conclusion

The Bouguer coherence method can only be used to provide estimates of $T_e$ where there is clear coherence between the free air gravity anomalies and topography, and may even then only provide an upper bound on the value. When $\gamma_f^2 \simeq 0$ neither the Bouguer coherence nor the admittance method can be used to estimate $T_e$. However, it is still sometimes possible to use the ratio of the power spectra of the free air gravity to the topography to put an upper bound on $T_e$. It is also sometimes possible to make an estimate of its value from profiles of the free air gravity.

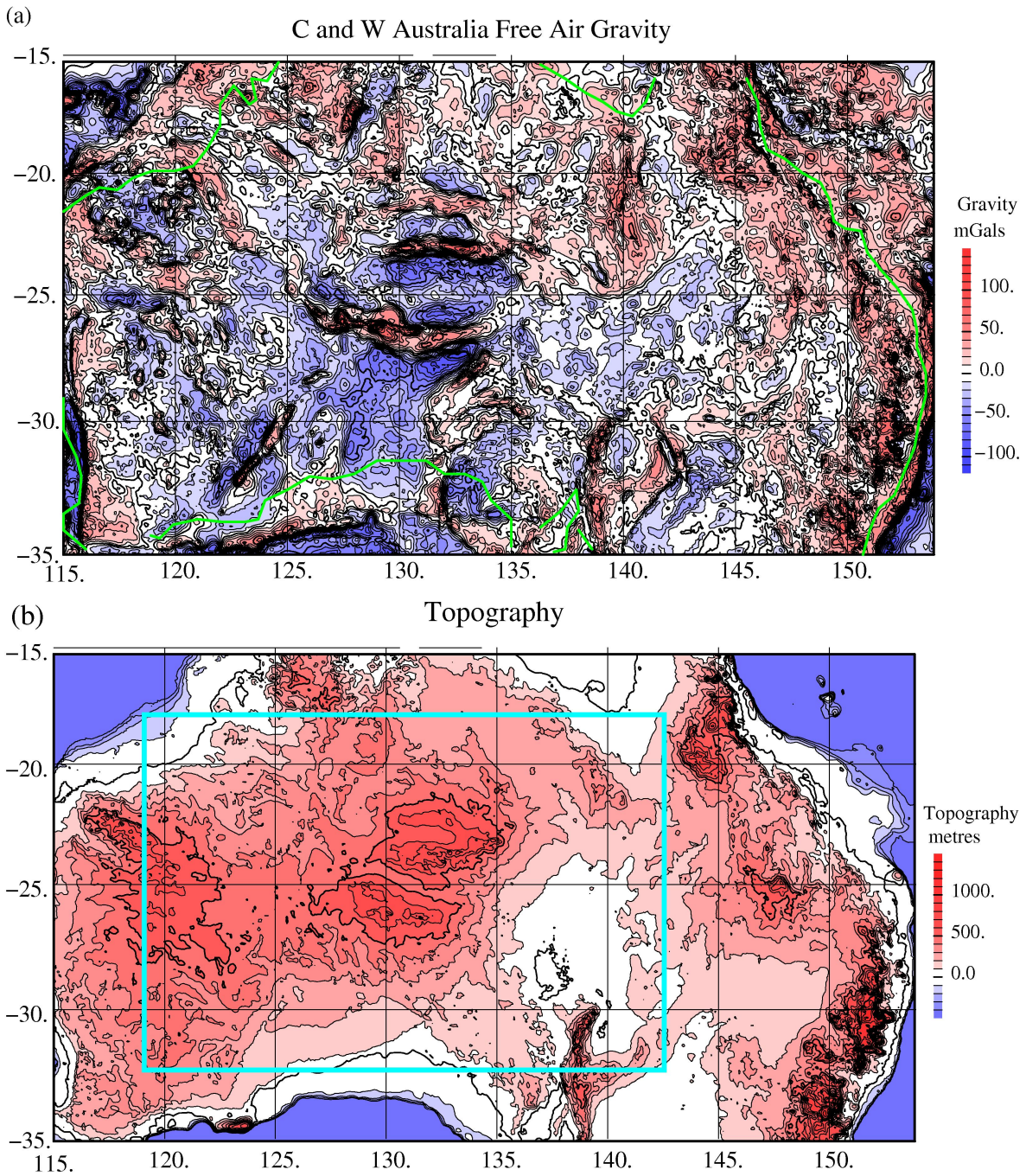


**Fig. 1** Free air gravity, (a), and topography, (b), of Australia. The blue box in (b) shows the region used to calculate the spectra of the topography and free air gravity.

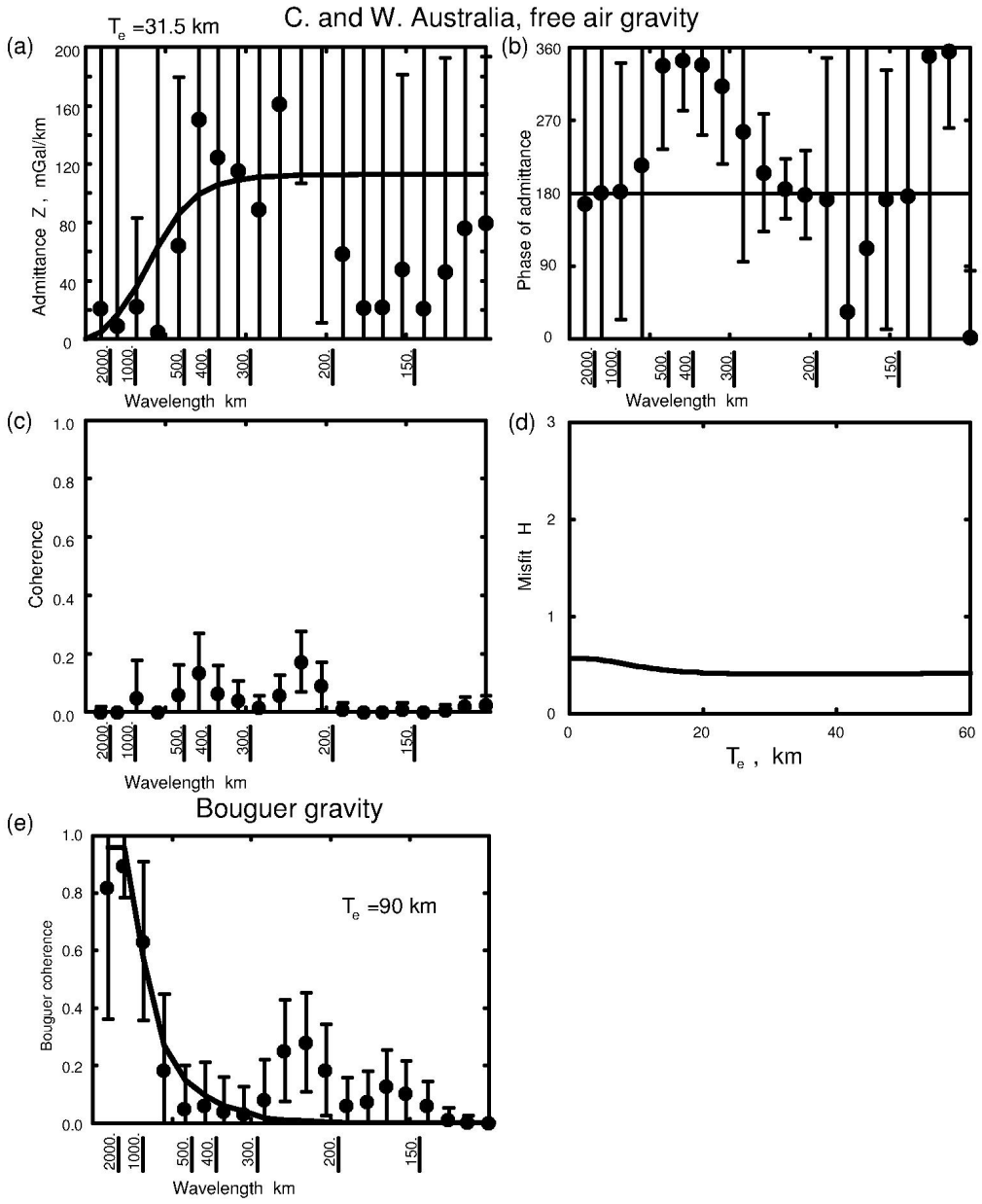


**Fig. 2** Amplitude, (a), and phase, (b), of the admittance within the box of Fig. 1b, using the topography as input, free air gravity anomaly as output. (c) shows the coherence between the free air gravity and the topography, and (d) the misfit (equation (4)) between the observed values of $|Z|$ and those calculated from equation (11) with $F = 1$. (e) Coherence between topography and Bouguer gravity for the region inside the box in Fig. 1b. The error bars show one standard deviation. The continuous line shows the behaviour expected when $T_e = 90$ km.

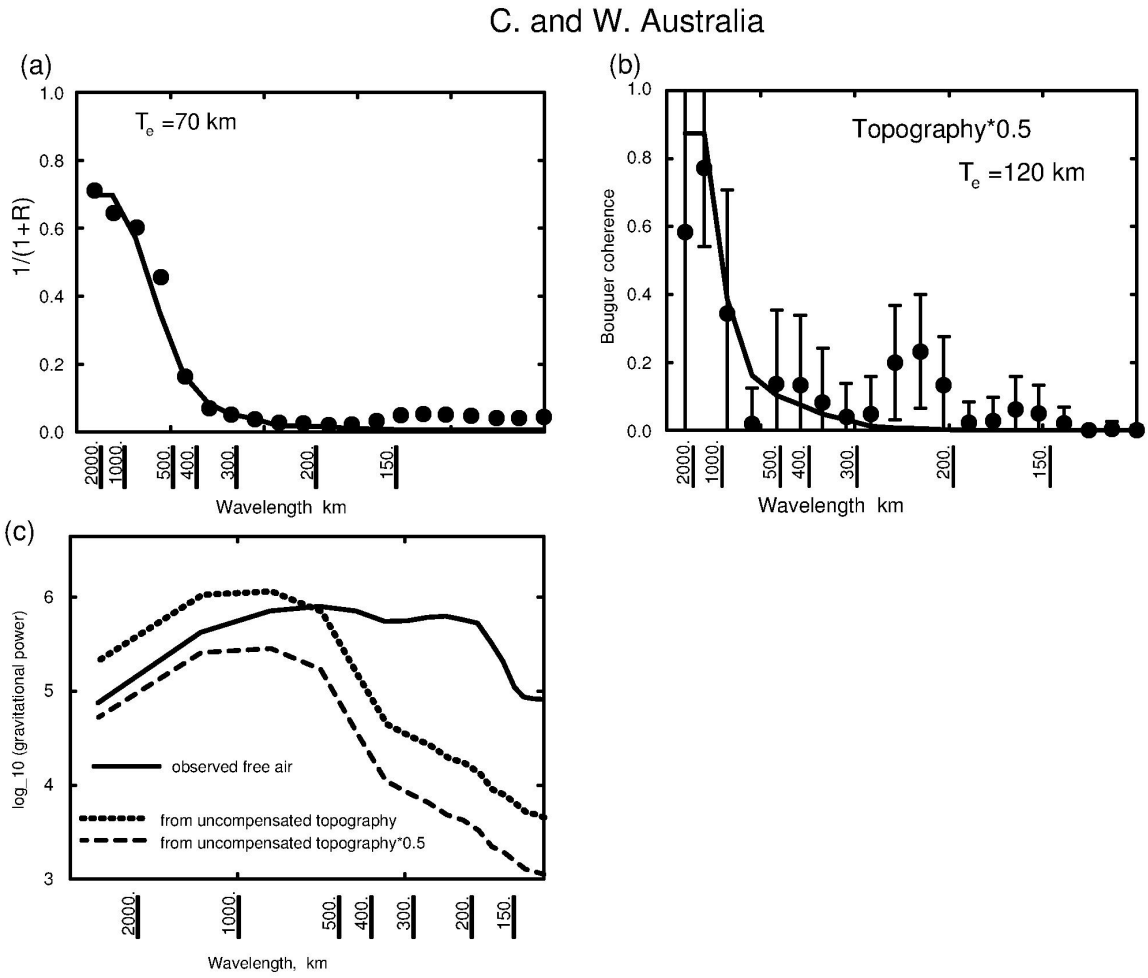


**Fig. 3** (a) $1/(1+R)$ (see equation (7)) calculated from the ratio of the power spectra of the free air gravity anomaly and that from uncompensated topography from the box in Fig. 1b. (b) as for Fig. 2e but with the topography reduced by a factor of 2. The units of the power spectra in this and other figures are $\mathrm{mGal}^2$ km

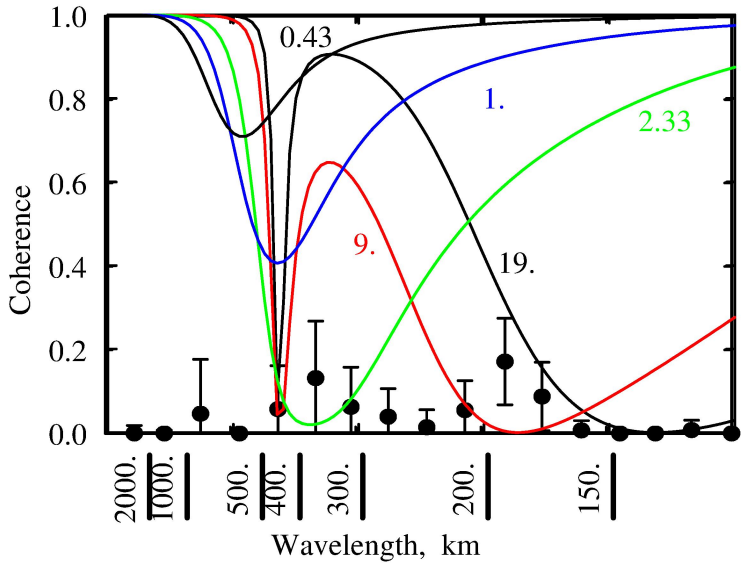


**Fig. 4** The curves show the free air coherence, calculated from Kirby's [5] expression with $T_e = 30$ km and marked with the values of $f$, the ratio of the subsurface to the surface load, which are assumed to be incoherent with each other. The solid dots show values from Fig. 2c.

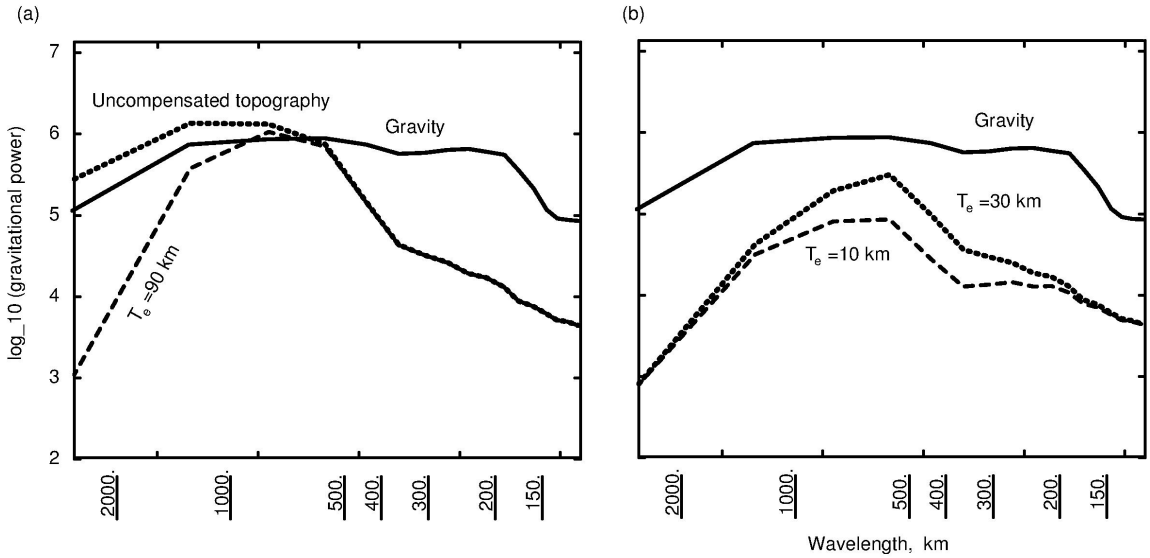


**Fig. 5** (a) Power spectra of the observed free air gravity anomaly, $g_f^o$, that $g_f^c$ expected from uncompensated surface topography, $At$, and from surface topography with $T_e$ = 90 km, for the box in Fig. 1b. (b) As for (a) but with $T_e$ = 30 and 10 km. The power spectra in all figures are in units of mGal$^2$ km.

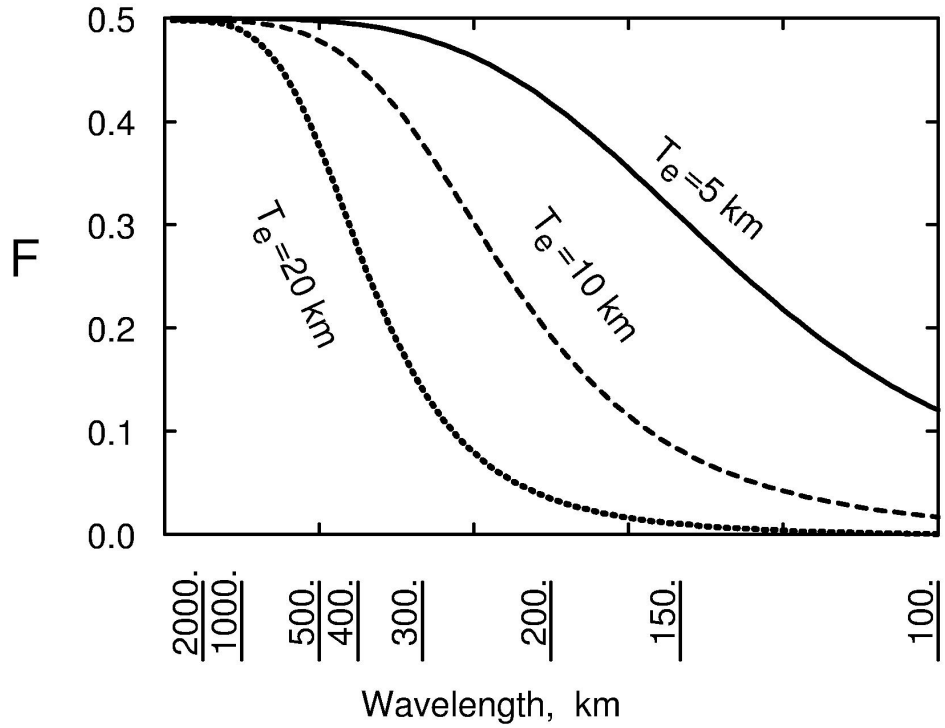


**Fig. 6** Values of $F$, the ratio of the surface to the total load (see equation (13) that generate no surface topography (see equation (16))

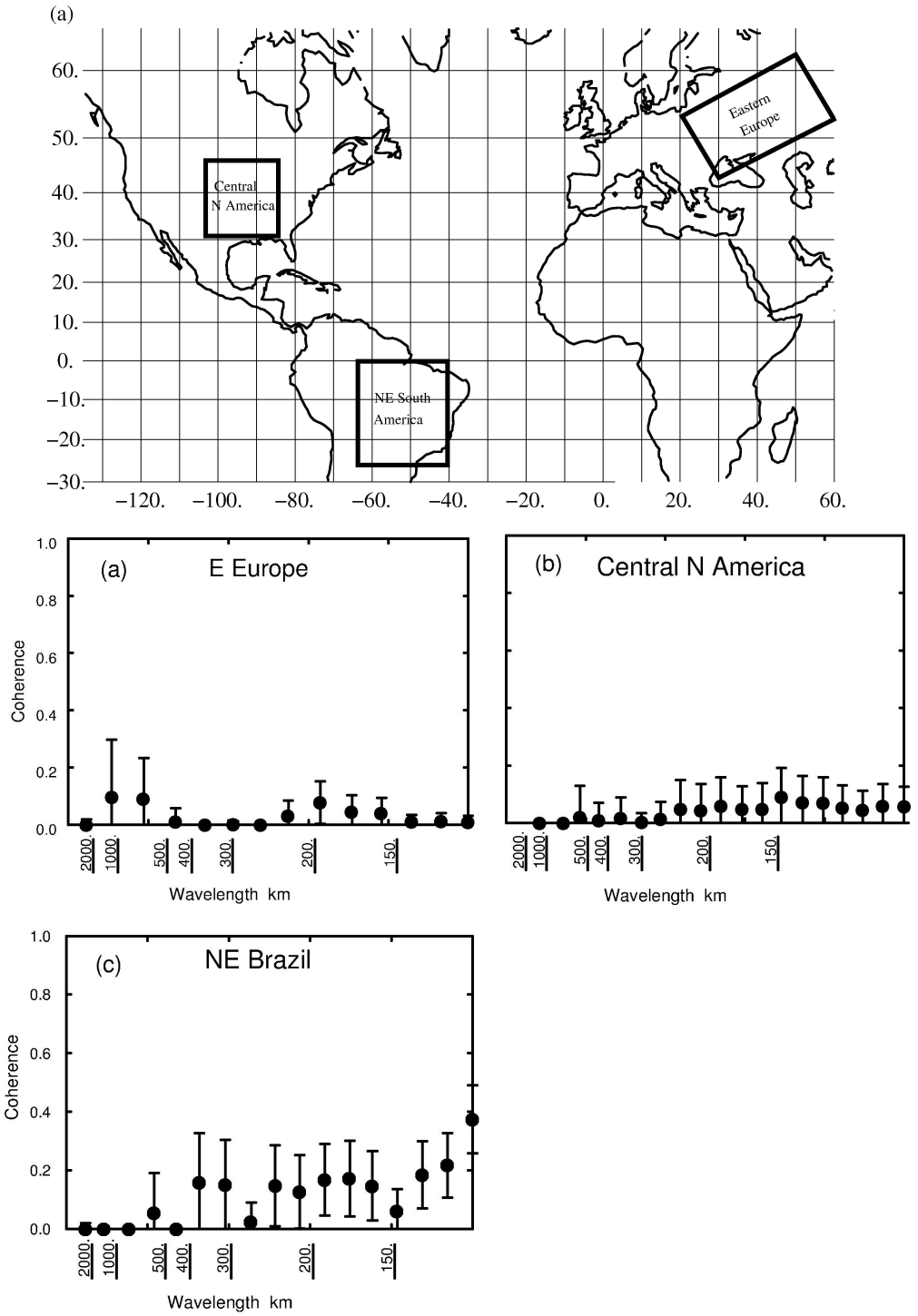


**Fig. 7** (a) Map showing regions used to calculate the coherence (b), (c), (d) between the free air gravity and topography.

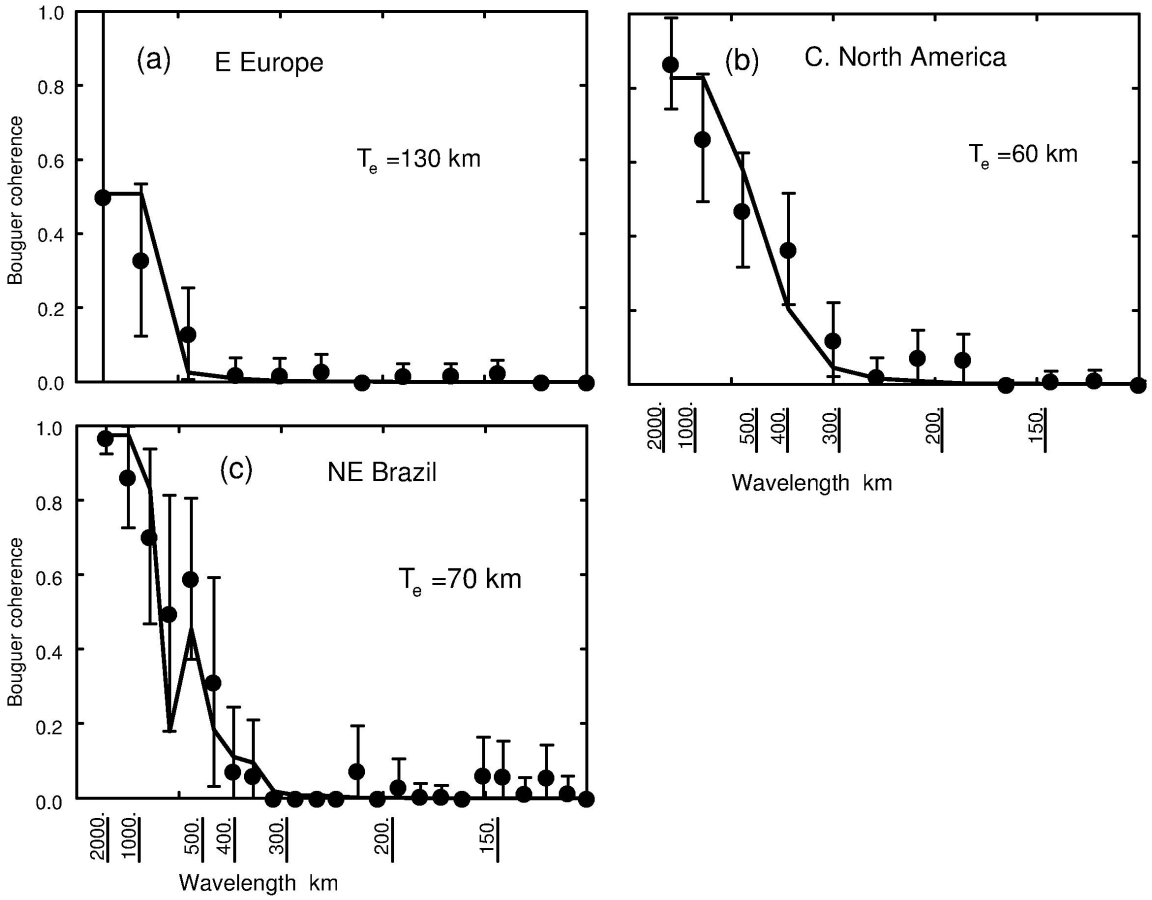


**Fig. 8** Bouguer coherence and resulting estimates of $T_e$ from the boxes in Fig. 7a.

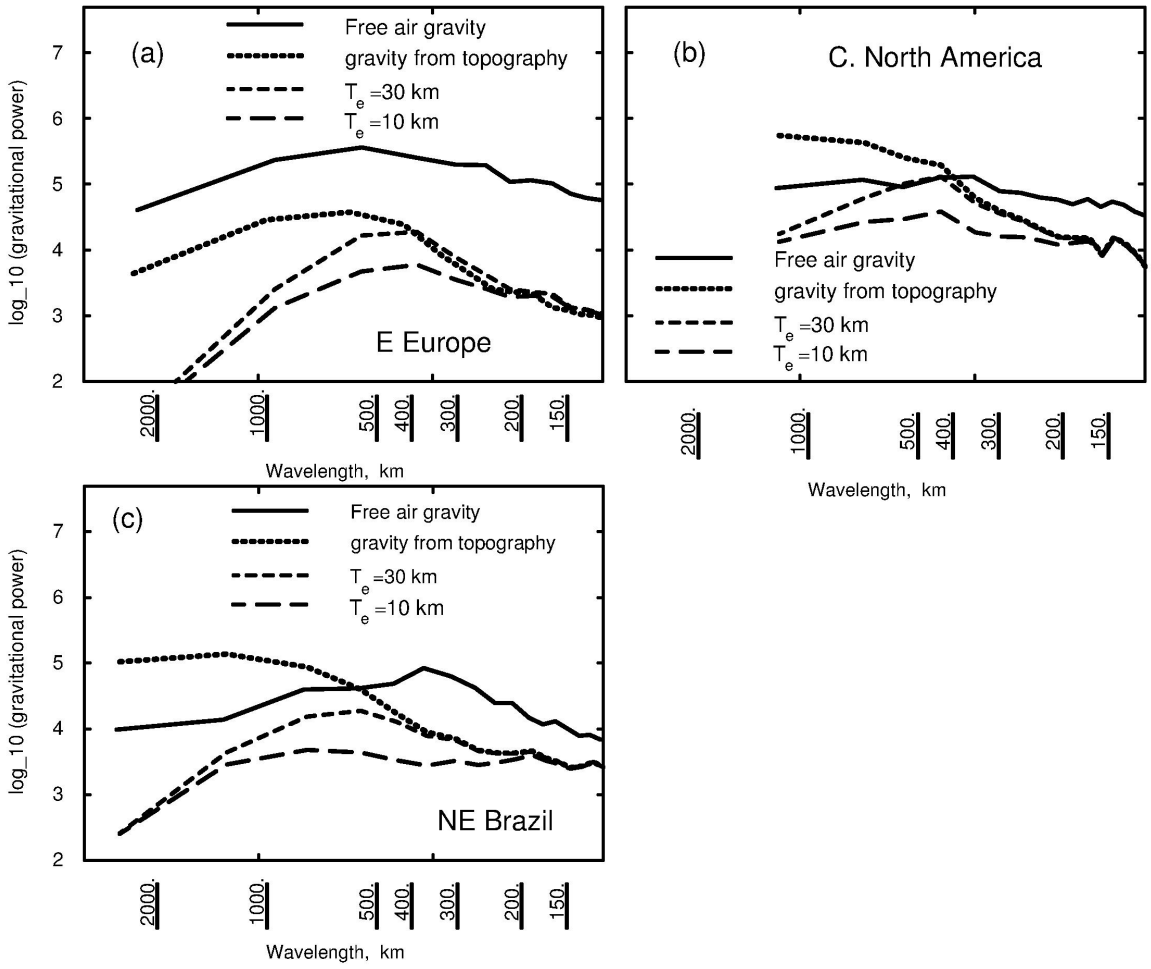


**Fig. 9** Power spectra of the free air gravity $g_f^o$, that $g_f^c$ from uncompensated surface topography $At$, and from surface topography with $T_e = 30$ and 10 km for the three boxes in Fig. 7a.

**Acknowledgements** I thank J. Jackson and F. Simons for their help and D. Forsyth for his detailed reviews.

## References

1. Banks, R.J., Parker, R.L., Huestis, S.P.: Isostatic compensation on a continental scale: local versus regional mechanisms. Geophys. J. Int. 51, 431-452. (1977)

2. Bechtel, T.D., Forsyth, D.W., Sharpton, V.L., Grieve, R.A.F.: Variations in effective elastic thickness of North American lithosphere. Nature, 343, 636-638. (1990)

3. Forsyth, D.W.: Subsurface loading and estimates of the flexural rigidity of continental lithosphere. J. Geophys. Res. 90, 12,623-12,632. (1985)

4. Jackson, J., McKenzie, D., Priestley, K. and Emmerson B.: New views on the structure and rheology of the lithosphere. J. Geol. Soc. Lond. 165, 453-465. (2008)

5. Kirby, J.F.: Estimation of the effective elastic thickness of the lithosphere using inverse spectral methods: The state of the art. Tectonophys. 631, 87-116, doi:10.1016/j.tecto.2014.04.021. (2014)

6. McKenzie, D.: Estimating $T_e$ in the presence of internal loads. J. Geophys. Res. 108(B9), 2438. doi 10.1029/2002JB001766. (2003)

7. McKenzie, D., Fairhead, J.D.: Estimates of the effective elastic thickness of the continental lithosphere from Bouguer and free air gravity anomalies. J. Geophys. Res. 102(B12), 27,523-27,552. (1997)

8. McNutt, M.K., Parker, R.L.: Isostasy in Australia and the Evolution of the Compensation Mechanism. Science, 199, 773-775. (1978)

9. Munk, W.H., Cartwright, D.E.: Tidal spectroscopy and prediction. Phil. Trans. R. Soc. Lond. Ser. A 259, 533-581. (1966)

10. Pérez-Gussinyé, M., Watts, A.B.: The long-term strength of Europe and its implications for plate-forming processes. Nature, 436, 381-384, doi:10.1038/nature03854. (2005)

11. Pérez-Gussinyé, M., Lowry, A.R., Watts, A.B.: Effective elastic thickness of South America and its implications for intracontinental deformation. Geochem. Geophys. Geosyst. 9, Q02003. doi:10.1029/2006GC001511. (2007)

12. Simons, F.J., Olhede, S.C.: Maximum-likelihood estimation of lithospheric flexural rigidity, initial-loading fraction and load correlation, under isotropy. Geophys. J. Int. 193, 1300-1342, doi:10.1093/gji/ggt056. (2013)

13. Watts, A.B.: Isostasy and flexure of the lithosphere. 458 pp Cambridge University Press, Cambridge, U.K. (2001)

14. Zuber, M.T., Bechtel, T.D., Forsyth, D.W.: Effective elastic thickness of the lithosphere and the mechanisms of isostatic compensation in Australia. J. Geophys. Res. 94, 9353-9367. (1989)